New β–decay spectroscopy of the ^{137}Te nucleus

M Si, R Lozeva, H Naïdja, A Blanc, J.-M Daugas, F Didierjean, G Duchêne, U Köster, T Kurtukian-Nieto, F Le Blanc, et al.

New $\beta-$decay spectroscopy of the ^{137}Te nucleus

M. Si(司敏),[1] R. Lozeva,[1,2] H. Naïdja,[3] A. Blanc,[4] J.-M. Daugas,[5,6] F. Didierjean,[2] G. Duchêne,[2] U. Köster,[4] T. Kurtukian-Nieto,[7] F. Le Blanc,[1,2] P. Mutti,[4] M. Ramdhane,[8] and W. Urban[9]

[1]*Université Paris-Saclay, IJCLab, CNRS/IN2P3, F-91405 Orsay, France*
[2]*Université de Strasbourg, IPHC, 23 rue du Loess, F-67037 Strasbourg, France*
[3]*Université Constantine 1, LPMS, DZ-25000, Constantine, Algeria*
[4]*Institut Laue-Langevin, F-38000 Grenoble Cedex 9, France*
[5]*CEA/DAM Île-de-France, F-91297 Arpajon Cedex, France*
[6]*Université Paris-Saclay, CEA, CNRS, Inserm, SHFJ, BioMaps, F-91401 Orsay, France*
[7]*CENBG, CNRS/IN2P3, Université de Bordeaux, F-33170 Gradignan Cedex, France*
[8]*LPSC, CNRS/IN2P3, Université de Grenoble Alpes, F-38026 Grenoble, Cedex, France*
[9]*Faculty of Physics, University of Warsaw, PL-02093 Warsaw, Poland*

(Dated: January 25, 2022)

Background: Nuclear structure of the neutron-rich isotopes beyond ^{132}Sn is investigated.
Purpose: The level scheme of ^{137}I is obtained after β decay of ^{137}Te. Transitions in ^{136}I are detected after β delayed neutron emission of ^{137}Te. The half life of ^{137}Te is measured.
Methods: β-delayed γ-ray spectroscopy is employed for neutron-rich ^{137}Sb and ^{137}Te isotopes, produced at the ILL after neutron-induced fission to populate excited states in ^{137}I.
Results: The new β decay level scheme of ^{137}I is established. The half lives of ^{137}Sb and ^{137}Te are determined as 0.57(26) s and 2.46(5) s, respectively. The β-delayed neutron emission probability P_n limiting value of ^{137}Te is deduced to be 2.17(66)%.
Conclusions: The experimental results are an important input to the theoretical description of nuclei in the region, being well interpreted within LSSM calculations and provide essential information on the first-forbidden transitions beyond $N > 82$ and $Z > 50$.

I. INTRODUCTION AND MOTIVATION

Close to the double shell closures in the nuclear chart with one of the good examples being the $^{132}_{50}Sn_{82}$ doubly-magic nucleus, the nuclear shell model stays a major structural framework to understand such magic nuclei and their neighbours. By investigating the nuclear configuration of states around the ^{132}Sn core, the extension of the magic core may be traced and the polarization effect of valence particles on the ^{132}Sn core may be studied in detail [1]. Valuable information on the nucleon-nucleon effective interaction and single-particle excitation energies may also be obtained. Furthermore, with increasing the neutron excess for these nuclei, a variety of new phenomena are predicted as the existence of neutron skin, vanishing of standard magic numbers or opening of new sub-shell gaps [2–5]. These phenomena challenge recent competitive studies and boost the quest for new data to more and more neutron-rich species. In our previous review on ^{136}Te which has two valence protons and two valence neutrons outside the doubly-magic ^{132}Sn core, deviations of the observed transition rates from the ones predicted by the shell-model calculation are found [6]. It is of great interest to investigate the Iodine isotopic chain, where in our review in [7] of ^{136}Te β decay, the excited levels of ^{136}I were established and compared to the shell model. In the present work new excited states also are identified in three valence protons systems beyond the magic number $Z = 50$. One of them, the ^{137}I nucleus, which has two valence neutrons outside the closed neutron shell $N = 82$ is of particular interest since also its low-spin excitations have not been explored in detail, while being very important for the nuclear structure in the region. Intermediate-spin states are addressed in our review on $^{135-139}$I nuclei [8].

The excess of valences particles could polarize the ^{132}Sn core and could lead to collective behaviour in ^{137}I, a quantity of information on the shell evolution of nuclei is expected at such extreme proton-neutron ratios. However, these I nuclei, similarly to their Te isotones, have not shown a very collective behaviour and a rather similar trend of excitation energies and transition rates of their first excited states [8] with the increase of N. The three valence protons in the Iodines [7] were also regarded as a cluster [9] to explain some features of these nuclei [10]. It is a very interesting exploration field though only the yrast states could be studied in both thermal neutron-induced ^{235}U-fission [11] and energetic neutron-induced ^{238}U-fission [8], while many of the non-yrast states could not be populated by this reaction. Based on the knowledge of the only previous β-decay work [12] with relatively scarce data on $A = 137$ as compared to its $A = 135$ isotope, only 5 excited states up to excitation energy of 1169 keV with 9 γ-ray transitions in ^{137}I were associated to the ^{137}Te decay scheme [13]. Therefore, new results on ^{137}I are highly demanded. More recently, benefiting from the development of experimental technology with radioactive neutron-rich beams [14–16], the majority of neutron-rich nuclei are investigated by spectroscopy of the fission products directly. In this work we report on the β decay of ^{137}Te, which is itself produced by the thermal neutron-induced fission reaction on ^{235}U.

II. EXPERIMENT

The exotic neutron-rich ^{137}Sb isotopes are produced at the ILL reactor, employing a thermal-neutron beam inducing fission onto a ^{235}U target. The projectile fission fragments of

interest are selected and identified by the LOHENGRIN [17] separator for two separate data sets tuned on A/Q setting for $Q = 21$ and $Q = 25$ to be able to disentangle more easily background from the radiation associated to the nucleus of interest. Further, the radioactive species are implanted onto our user detection system for a decay type of measurement. The detection setup consists of the LOENIE [18] $\beta-$decay station of plastic detectors in 4π geometry, placed around a supported movable Al-coated Mylar tape, evacuating the radioactivity from the implanted ions.

The measurement cycle is adapted to the half life, $T_{1/2}$, of the isotopes of interest. In this work, the time chopper is set to 3 s for injection, 3 s for measurement and 2 s for tape movement. This information is further used to extract the experimental $T_{1/2}$ value (see Sec. III A). Prompt and β-delayed γ rays emitted from the implanted isotopes could be detected by two Clover detectors (with Anti-Compton (AC) shields, used as passive shielding) and a coaxial HPGe detector in a very close geometry. Data is collected by a standard triggerless VME electronics. Further experimental details, including information on the γ-ray detection efficiency are given also in Ref. [19]. As appropriate for the studied energy range, these were also cross-checked with the experimental relative efficiencies of the $A = 136$ daughter nuclei [7].

For the $A = 137$ study reported here, it is relevant to state, that isobars and long-lived contaminants as ^{137}I, and ^{137}Xe (and ^{142}Ba in $Q = 25$ case), produced directly in fission may also reach the experimental station, as the LOHENGRIN separator does not distinguish between isobars abundant quantities of the longer-lived isobars. Such activities are taken into account in the analysis as they are already well known and mostly contribute as a long-lived background.

III. DATA ANALYSIS AND RESULTS

A. Half life of ^{137}Te

Due to the very short half-life of the implanted ^{137}Sb ions and its exoticity with respect to the daughter products, the delayed spectra are dominated by these ^{137}Te, ^{137}I daughter/grand-daughters. Also, as explained above such $A = 137$ contamination is present in the initially-implanted ions as they are produced stronger in the fission. The γ-ray energy after β decay and the corresponding timing information, based on the beam chopping are used to construct the "time chopper-energy" matrix. This matrix allows to monitor the activity of γ-rays within the measurement cycle itself. By gating on β-delayed γ-rays in ^{137}I, we obtain the decay curve of ^{137}Te. To demonstrate this and in order to increase the statistics, we summed up the time distributions of already known γ-rays in this nucleus as 129 keV, 243 keV, 469 keV and 554 keV and fitted the half life using minimization procedure. As shown in Fig.1, the contribution of the daughter ^{137}Te is dominating the time curve. While any ^{137}Sb contribution is minor (weakly produced and shorter) and may be neglected, the grand-daughter ^{137}I nuclei may contribute to the background and can be accounted either directly with the known $T_{1/2}$ in the Bateman equations fitting [20], or as a long-lived activity background with very similar outcomes. The resulting β-decay $T_{1/2}$ are reported in Table. I together with the values from previous measurements [13]. The uncertainty in the current results comes from the statistical error and the fitting. The result on the ^{137}Sb comes from the limit of this observation which is the 61.8 keV line (Fig. 2), corresponding to the deexictation of the excited state in ^{137}Te. We have to note however, that it can be still polluted by some unidentified origin as we could not observe any coincidence transitions, e.g. those reported in Ref. [21], possibly due their much lower intensity and the overall low production of ^{137}Sb. Thus, the result can be taken as an experimental limit justifying an agreement with previous observations.

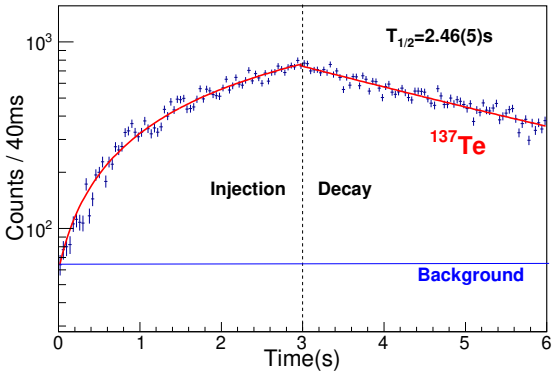

Figure 1. Time distribution of ^{137}Te β-decay events fitted with the resulting half-life.

Table I. β-decay half-lives measured in this work compared with literature values

nucleus	$T_{1/2}^{exp}$ (s)	$T_{1/2}^{lit}$ (s)
^{137}Sb	0.57(26)	0.566(52) [22], 0.492(25) [22],0.507(27) [21]
^{137}Te	2.46(5)	2.49(5) [12], 2.1(1) [23], 2.08(40) [24]

B. ^{137}Te β decay to excited states in ^{137}I

In the previous $\beta - \gamma$ spectroscopic study of ^{137}I, 5 excited levels and 9 γ transitions were established [13], far below the Q_β value of 7053(9) keV (see Sec. III D). In the present work, β-delayed γ-ray spectrum of ^{137}I is obtained by applying β-β coincidence conditions to all Ge data. The β-gated γ-ray spectrum for different A/Q settings on $Q = 21$ and $Q = 25$, as taken in our measurement, is shown in Fig.2. One can clearly see, as marked by their energies, that in both settings the transitions from ^{137}I are well identified. The main background comes from the ^{137}Xe grand-daughter nuclei, while for $Q = 25$, also ^{142}Ba contributes to the background. In order to subtract the background from long or short-lived nuclei, the analysis are performed under the condition that the selected time window corresponds to the chopper decay part (see Fig. 3). Transitions

from the previous measurements, β-decay of ^{137}I [12] and fission [8, 11] are observed in this work.

With the aim to expand and establish a new level scheme of ^{137}I from this new β decay data, β-γ, γ-γ (mutual) coincidences and γ intensity balances are used. The γ-γ coincidence relations are constructed between the Clover detectors and the coaxial HPGe detector. For all these, we also used a coincidence with the detected β signal to suppress the prompt γ-ray background (similar information is given also in Ref. [19]). In Fig. 4, we show a spectrum gated on the 243.6-keV, transition corresponding to the the first excited state in ^{137}I, where 15 cases of mutual coincidences could be found. Four of them are consistent with the previous knowledge: 129.5 keV, 357.2 keV, 469.7 keV and 925.9 keV, while six of them are used to construct six new excited levels: 609.6 keV, 974.4 keV, 1155.4 keV, 1833.7 keV, 2047 keV and 2170.2 keV. In Fig.2, the 974.4 keV γ peak sits on the tail of a background γ in the Q = 25 (red) spectrum and is thus weak in the Q = 21 (blue) spectrum. As it has a very strong mutual coincidence with the 243.6 keV γ-ray, we propose to place this transitions on the top of the known 243.6-keV level. Due to weak statistics, for the 1833.7 keV, 2047.1 keV and 2170.2 keV transitions we present, in addition, their gated spectra, illustrated in Fig.4. The weakly seen 2047 keV γ-ray in Fig.2, is marked as tentative. The new 227.1-keV transition, found in the 243.6 keV gated spectrum, shown in Fig.4, is also in coincidence with the 229.1-keV line (in the 227 keV gated spectrum, see Fig. 6), and all transitions de-exciting the level 373.1 keV such as the 129.5-keV line). As its energy, in addition, fits the energy difference between the 600.6-keV and 373.1-keV levels, we place it as a new transition in the level scheme (see Fig. 7). The 229.1-keV line is proposed to be on the top of the 600.6 keV state, establishing a new level with energy of 830.2 keV. This new level is connected also with 554.2 keV state by the new 276.2 keV transition that can also be traced in the coincidence relations depicted in Fig. 4.

The 554.2-keV level has previously been observed in the fission reaction studies [8, 11], with a single de-excitation by one transition to the ground state (g.s.). One can see from Fig.4, that the 554.2 keV gated spectrum provides 5 mutual coincidence lines. The 440.9 keV γ transition is known from the previous fission works to connect with the higher-lying (13/2$^+$) state. The 276.2 keV, 299.0 keV and 897.7-keV lines are observed for the first time here. The 276.2-keV transition fits the energy difference between the new excited level at 830.2 keV and the 554.2 keV, proves the existence of new connections with energies of 830.2 keV, 299.1 keV and 897.7 keV, and provides an evidence in establishing the new excited levels at 853.2 keV and 1451.9 keV excitation energy. These two levels can also be cross-checked inspecting their connections to the other levels. The 600-keV transition is marked as tentative as it is difficult to be distinguished from the de-excitation of the 600.6 keV level to g.s.. The 1170.1-keV level is known previously because of its mutual coincidence with the 925.9-keV and 243.6-keV transitions. Three other transitions de-excite this level as observed in this work, and they are weaker than the 925.9 keV line. The 569.5 keV gated spectrum, illustrated in Fig.6, shows these coincidence transitions and suggests that the 569.5 keV line can be placed on the top of the 600.6 keV level and its energy fits well the energy difference between these 1170.1 keV and 600.6 keV states. Therefore, it is assigned to the de-excitation of level 1170.1 keV to level 600.6 keV.

Another previously-known transition which we observe here has the energy of 620.5 keV and is assigned to de-excite the 620.5-keV level directly to the g.s., without any connections to the other levels. As we could not identify any coincidence relations with known transitions, we use the time chopper information to obtain its time behaviour. The principle of this method is to use the time-energy matrix, by projecting the energy spectrum for every 1 s within time chopper decay part and thus trace the transition timing within the correct $T_{1/2}$ of the nucleus of interest. Fig.5-(a) shows how the known 243.6-keV transition behaves as an example, while the 1435.9 keV-transition is assigned as a new transitions regarding this criteria. Fig.5-(c,d) show how transitions from the daughters ^{137}Xe and ^{137}Cs behave. Due to their long $T_{1/2}$ the statistics within the decay part remains basically the same for these time projections. This criteria is used to cross-check all the new transitions observed in singles or in gated spectra and helps to reject wrongly suspected candidates.

To assign new transitions to the level scheme of ^{137}I we used the following criteria: a) the same timing; b) mutual coincidence relations with known or new transitions; c) the same relative intensity in Q = 21 and Q = 25 settings; d) not identified to the background or the contaminants. According to these criteria, 17 excited levels could be established in this work with a total of 32 γ-ray transitions following the β decay of ^{137}Te to ^{137}I. Among these, we observe for the first time 8 new and one tentative levels with 18 new and two tentative transitions. Table. II summarizes the information about the excited levels and γ transitions associated with this β decay to the ^{137}I nucleus. The γ-rays intensities are normalized to the strongest 243.6-keV transition, and obtained using the background subtracted full-energy peak areas from β-gated γ-ray spectrum selecting the time chopper decay part. The β intensity of each level is extracted from the feeding and decaying γ transitions of this particular state. Its log ft value is calculated using the Q(β^-) = 7053(9) keV from the atomic mass evaluation (AME2020 [25]) and Ref. [26].

C. ^{137}Te β feeding to the ^{137}I ground state

In order to obtain the ^{137}I β feeding, its further decay to ^{137}Xe and its P$_n$ channel to ^{136}Xe are considered. As there is no long-lived (e.g. ms) isomeric state in ^{137}I, these are the two branches representing the total g.s. feeding of ^{137}I. For the β decay to ^{137}Xe, g.s. to g.s. transitions as well as excited states are taken into account.

We observed 34 excited states and 43 γ transitions in ^{137}Xe by the g.s. β decay of ^{137}I, representing about 80% of the known transitions in ^{137}Xe [13]. The I$_\beta$ for the g.s. of ^{137}Xe is obtained in the same way: considering the β feeding from the ^{137}Xe g.s. to ^{137}Cs. For the β-n channel of ^{137}I we did not observe known transitions in ^{136}Xe. Note that the latest P_n value is 7.76(14)% [27], compared to the evaluated one

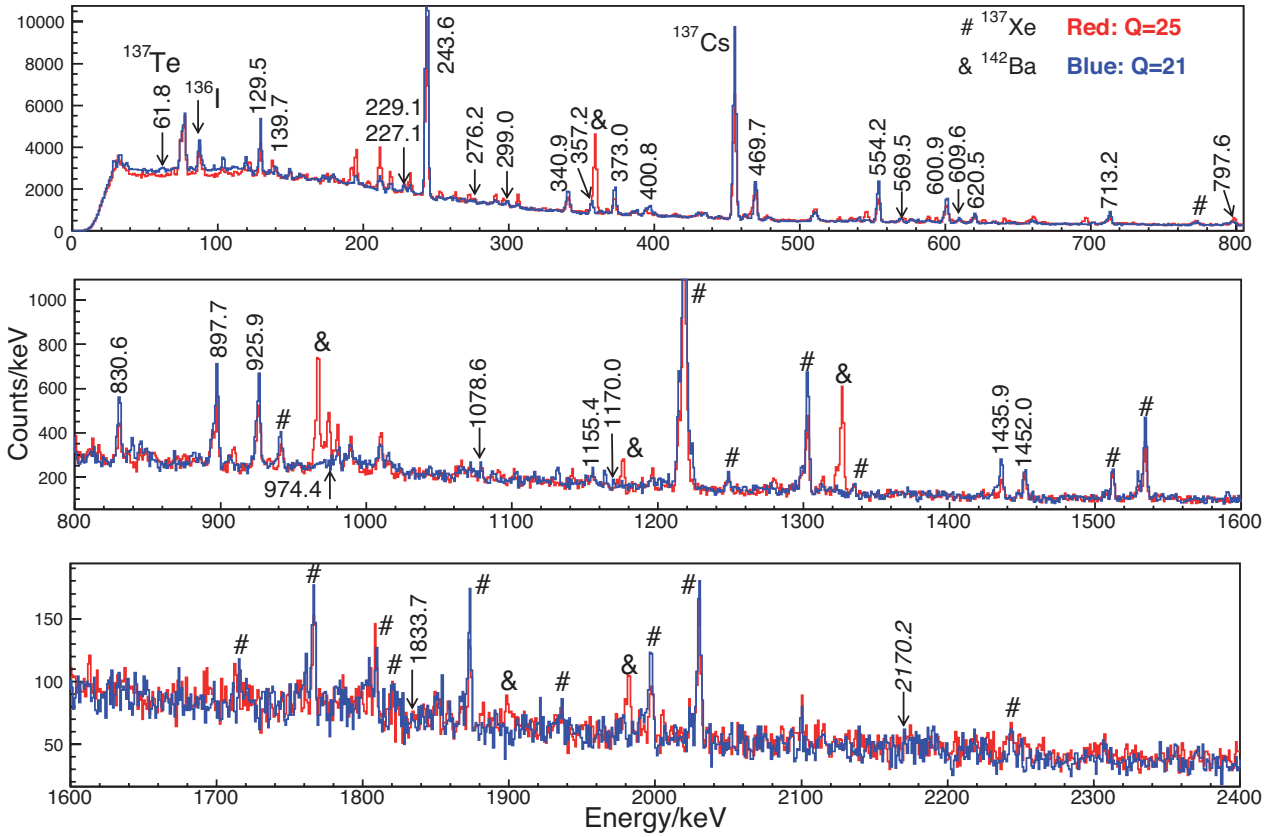

Figure 2. The β-gated γ-ray singles spectrum obtained following the β-decay of ^{137}Te for both Q settings. Peaks belonging to ^{137}I are marked by their energies. The main background comes from ^{137}Xe grand-daughter nuclei and a ^{142}Ba contaminant for Q = 25.

of 7.14(23)% [13]. Combining the above information, except correcting for unobserved branches in the daughter and unobserved P_n-related γ-ray in Xe, we estimated in addition the real production of ^{137}Xe in the γ-spectrum of the ^{137}Te decay in the following way. The counted γ-rays belonging to Xe in the 3-6 s decay part, corrected for nonobservance are compared to those in the 0-1 s of the Te decay, where only 3% follows decay (due to its $T_{1/2}$). Analysing these portions showed that the γ-rays from Xe in this time range correspond to 20% of those in the entire decay and thus one may infer that 80% of the Xe actually comes from the Te decay and 20% is from direct production. Therefore, correcting for the above factors, the total error for the I$_\beta$ g.s. feeding rises of up to 22% as reported in Table II. This reflects also the experimental log ft uncertainties of particular levels as a systematic error, while the statistical errors contribute to below or around the percent level in this measurement. It may be noted also that as several transitions in A = 137 are in the energy range relevant for conversion, this is also investigated. While some of these transitions, as the 243.6 keV the multipolarity comes from previous measurements [11, 28], for the others, the possible $M1$ and $E2$ assumptions can be made. However, while most of these transitions are weak in intensity and their proportion is found to be minor, for two relevant γ-rays of 129.5 keV and 139.7 keV, the conversion factors assuming the four different combinations changes the relative I_β of the level. For example, for the 243.6 keV level the I_β uncertainty increases from 12.8(2.8) to 12.8(3.7). This is relevant also for the 373.1, 713.5 and 853.2 keV levels and as the change is internally in the ^{137}I level scheme, it does not affect the g.s. feeding and thus its uncertainty.

D. Level scheme and spin-parity assignments

Due to the 7/2$^-$ spin/parity of the parent nucleus, only the low-spin states are expected to be observed in its β decay, taking into account the predominant forbidden nature of these transitions. The g.s. spin/parity of ^{137}I as its daughter as 7/2$^+$ is established earlier and completely consistent with our work here (see Sec. IV for details). For the 620.5 keV state, the spin/parity of 11/2$^+$ was set because of the deduced $E2$ transition multipolarity of the 620.5 keV γ-ray in the spontaneous fission data [11]. In that study the angular correlations of this line were regarded with respect to the 333.9 keV line connecting the suggested 13/2$^+$ level at 955.0 with the proposed 11/2$^+$, assumed as an $M1 + E2$ type.

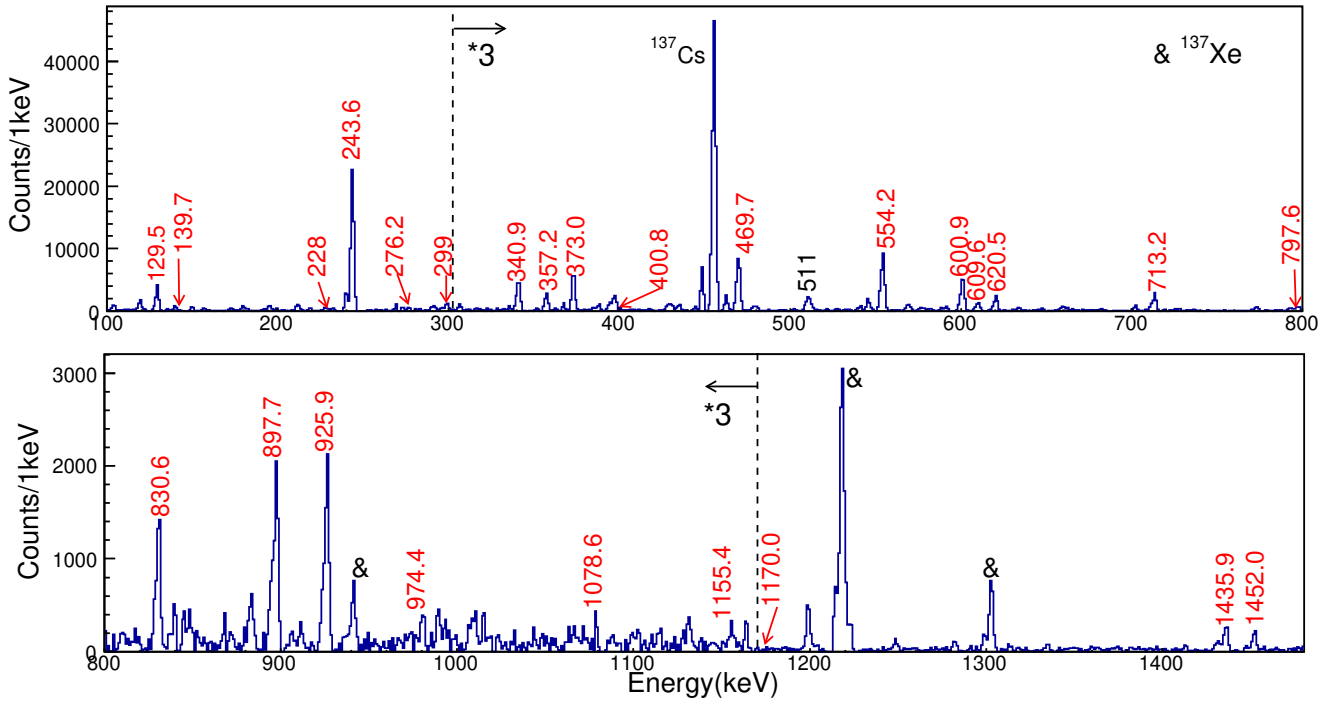

Figure 3. The β-gated γ-ray singles spectrum obtained following the β-decay of ^{137}Te, after background subtraction for Q = 21. The leftover from the background is from ^{137}Xe.

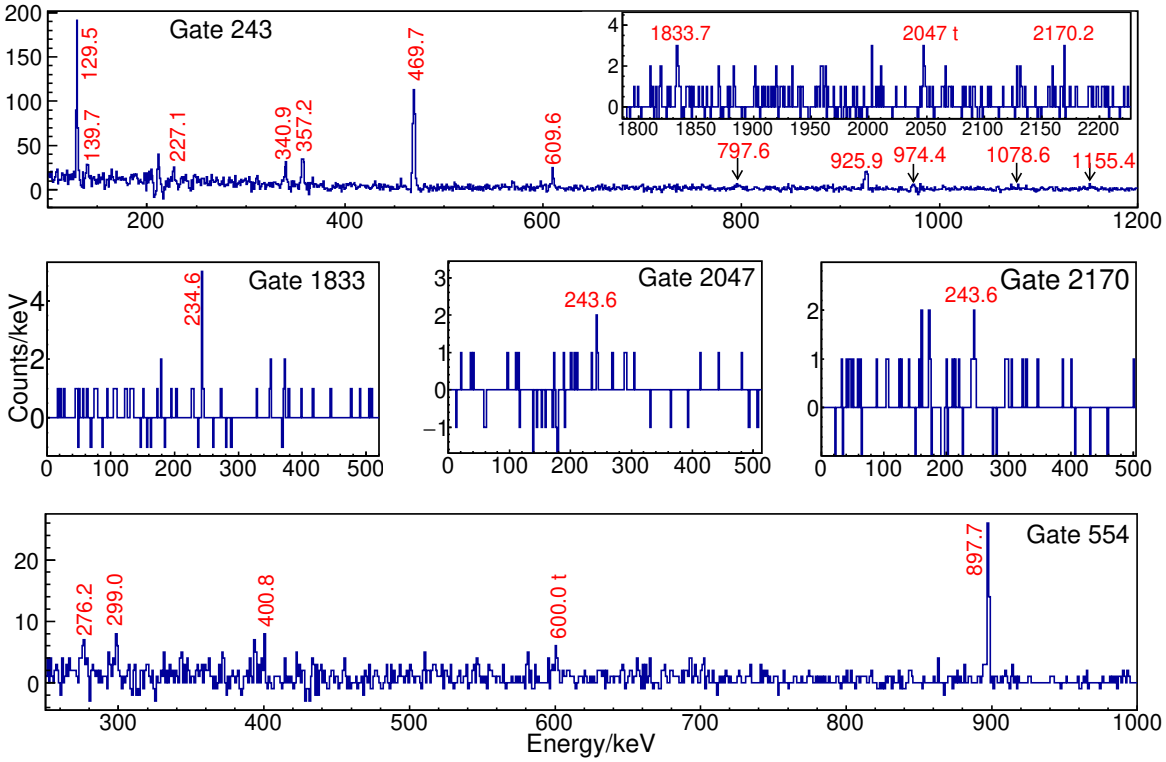

Figure 4. Coincidence γ-ray spectra gated on different transitions. All marked peaks are in mutual coincidence.

Table II: Excited levels and γ transitions in the β decay of ^{137}Te to ^{137}I. The initial level and its related information are given in the first four columns. The γ ray and its absolute intensity are provided in the fifth and sixth columns. The last two columns reveal the final level and its spin/parity. The superscript n stands for a new transition, while u marks also an assumption for uniqueness [26].

E_i(keV)	J_i^π	I_β(%)	log ft	E_γ(keV)	I_γ(%)	E_f (keV)	J_f^π
0.0	$7/2^+$	47(10)	5.7(1)				
243.6(8)	$5/2^+$	12.8(37)	6.2(1)	243.6(8)	100.0(6)	0	$7/2^+$
373.1(7)	$(3/2^+,5/2^+)$	2.8(14)	6.9(2)	129.5(7)	12.2(2)	243.6	$5/2^+$
				373.0(9)	15.2(3)	0	$7/2^+$
554.2(10)	$9/2^+$	7.0(15)	6.4(1)	554.2(10)	33.4(5)	0	$7/2^+$
600.6(6)	$(3/2^+,5/2^+)$	2.4(6)	6.9(1)	227.1(7)^n	1.2(1)	373.1	$(3/2^+,5/2^+)$
				357.2(10)	6.1(2)	243.6	$5/2^+$
				600.9(10)	4.1(2)	0	$7/2^+$
620.5(10)	$9/2^+,11/2^+$	2.5(6)	6.8(1)	620.5(10)	8.9(3)	0	$7/2^+$
713.5(7)	$(7/2^+)$	14.8(33)	6.0(1)	340.9(11)	13.3(2)	373.1	$(3/2^+,5/2^+)$
				469.7(9)	26.1(4)	243.6	$5/2^+$
				713.2(12)	13.7(3)	0	$7/2^+$
830.2(6)^n	$(5/2^+,9/2^+)$	1.5(3)	7.0(1)	229.1(7)^n	1.2(1)	600.6	$(3/2^+,5/2^+)$
				276.2(5)^n	0.3(1)	554.2	$9/2^+$
				830.6(11)^n	3.7(2)	0	$7/2^+$
853.2(7)^n	$(5/2^+,9/2^+)$	1.5(3)	7.0(1)	139.7(6)^n	0.9(1)	713.5	$(7/2^+)$
				299.0(11)^n	2.2(1)	554.2	$9/2^+$
				609.6(10)^n	2.0(1)	243.6	$5/2^+$
955.0(12)	$11/2^+,13/2^+$	0.3(1)	7.6-9.6^u	400.8(7)	1.1(1)	554.2	$9/2^+$
1170.1(6)	$(7/2^+)$	2.9(7)	6.6(1)	569.5(9)^n	1.6(1)	600.6	$(3/2^+,5/2^+)$
				797.6(10)^n	2.1(1)	373.1	$(3/2^+,5/2^+)$
				925.9(12)	5.5(2)	243.6	$5/2^+$
				1170.0(7)^n	0.8(1)	0	$7/2^+$
1218.0(11)^n	$(3/2^+,9/2^+)$	0.3(1)	7.6(1)	974.4(8)^n	1.1(1)	243.6	$5/2^+$
1399.0(11)^n	$(3/2^+,11/2^+)$	0.2(1)	7.7-9.6^u	1155.4(8)^n	0.7(1)	243.6	$5/2^+$
1435.9(9)^n	$(5/2^+,9/2^+)$	0.8(2)	7.1(1)	1435.9(9)^n	2.8(2)	0	$7/2^+$
1451.9(7)^n	$(7/2^+)$	2.5(6)	6.6(1)	600^t		853.2^n	$(5/2^+,9/2^+)$
				897.7(9)^n	5.0(2)	554.2^n	$9/2^+$
				1078.6(8)^n	1.1(1)	373.1	$(3/2^+,5/2^+)$
				1452.0(11)^n	2.7(2)	0	$7/2^+$
2077.3(14)^n	$(3/2^+,11/2^+)$	0.1(1)	7.7-9.5^u	1833.7(11)^n	0.3(1)	243.6	$5/2^+$
2290.6(14)^t				2047^t		243.6	$5/2^+$
2413.8(12)^n	$(3/2^+,9/2^+)$	0.2(1)	7.3(1)	2170.2(9)^n	0.7(1)	243.6	$5/2^+$

The 620.5 keV state, observed in this work represents a single transition to the ground state. However, we could not detect any coincident transitions to represent feeders from above. Thus, its intensity should be mostly coming in direct β feeding. Such scenario would not be entirely consistent with an earlier proposed spin/parity of $11/2^+$ and log ft value of 6.8(1) evaluated in this work, therefore according to our data $\Delta J < 2$ possibility shall not be excluded. For example, if the presumed $11/2^+$ level would be a $9/2^+$ candidate, the 620.5-keV transition may have some mixing and this would not conflict several deviations from the theoretical angular correlation coefficients from the previous observation in Ref. [11]. Such scenario would include the margin in the β intensity, observed in this experiment and respectively may be also suggested for the 620.5-keV level.

The 554.2-keV [13] state was set to $9/2^+$ based on the suggested mixed $M1+E2$ multipolarity of the 554.2-keV transition, observed in Ref. [11], with respect to the 400.8-keV transition. Both were placed in the level scheme in coincidence, that we indeed also observe in Fig. 4). Similarly, if the 400.8-keV transition would originate from a $11/2^+$ instead of the $13/2^+$, suggested for the 955.0 keV level, some possible mixing due some deviations in angular distribution, polarization data or alternation of spins may need to be assumed. In this experimental data, due to visible I_β intensity and relatively well fitting log ft values, the previously assigned $11/2^+$ and $13/2^+$ states are now given possible alternative assignments in the level scheme, shown in Fig. 7 and Table II.

As we detect the 554.2-keV transition as the second strongest, relative to that of the first excited state (also previously identified with spin/parity of $5/2^+$ [12]), this gives quite some certitude for the spin of the originating state. It does well fit the spin/parity of $7/2^+$ for the g.s. and is in a very good agreement with our shell-model (SM) expectations (see Sec. IV) that places the first $9/2^+$ state at 554.2 keV excitation energy. Furthermore, looking at the I_β and log ft values for the 554.2-keV level, some $5/2^+$ possibility cannot be completely excluded. This tendency actually comes from the fact

that if the 554.2-keV transition is mostly an $M1$ type, mixed with some $E2$ multipolarity, the required $\Delta J = 1$ branch would connect similarly strong a $5/2^+$ to the $7/2^+$ ground state. Note that the SM calculations (see Sec. IV) predict, that the second $5/2^+$ state may be expected much below the first $9/2^+$ state and such a state would be populated directly and relatively strongly from the $7/2^-$ g.s. β decay.

The next candidate for the second $(7/2^+)$ state is the previously observed 713.5 keV state, de-exciting by three γ transitions, that we also observe, with the strongest one connecting to the 243.6 keV state with a spin/parity $5/2^+$ Ref. [11, 12]. Its experimental I_β and log ft also suggest $(7/2^+)$ assignment. However, such identification would be somewhat in variance with the SM prediction that expects the second $7/2^+$ level at 571 keV excitation energy, while the third $7/2^+$ state is calculated at 774 keV (see Sec. IV). Although they all are predicted with the same configuration, there is no clear reason why they would be compressed, except the possibility of unaccounted mixing in the configuration of these states. The third candidate for such spin/parity, according to our data, is at excitation energy of 1170.1 keV. This is very well probable and matches the findings of Ref. [12] to our data, where we observed three more transitions de-exiting this level (see Fig. 7). The level must have been among the strongest ones observed in that first β-decay study and their proposed spins as $5/2^+$ and $7/2^+$ would be the favoured ones from the $7/2^-$ g.s. of the mother nucleus, thus very consistent.

The two levels at 830.2 keV and 853.2 keV have similar I_β and log ft values though lower than expected for spin/parity of $7/2^+$. Besides, their interconnecting transitions to the lower-lying $5/2^+$ and $9/2^+$ states, make this $7/2^+$ possibility less adequate. Therefore, we propose both $(5/2^+,9/2^+)$ as spin/parities assignments. This would agree with the SM results for $9/2^+$ and be underestimated for a $5/2^+$, while the third $7/2^+$ and $3/2^+$ states, expected in the vicinity at 774 keV and 900 keV, require different experimental branching.

The next level which experimentally has strong I_β feeding and can be the $(7/2^+)$ state is located at 1170.1 keV, previously observed and matching the forth $7/2^+$ predicted at 1085 keV. The state at 1451.9 keV which has similar characteristics may have the same origin, thus also proposed as a $(7/2^+)$ state. Although the $(5/2^+)$ possibility cannot be completely excluded this would require more data to search for feeding branches that we could not observe. Interestingly, the five states we suggest with spin/parity $5/2^+$ or $7/2^+$ ($E_x < 1.2$ MeV), being the strongest fed, are communicated though left unassigned in Ref. [12].

In the data presented here, it can be seen that four similar new excited states at 830.2, 853.2, 1435.9 and 1451.9 keV are established. According to their possible de-excitation transition multipolarities, the spin/parities are consistent with the earlier proposed $(9/2^+)$ spin/parity, while due to the relatively low log ft value a $(5/2^+)$ possibility may be added or even $(7/2^+)$ for the later one.

Some spin-parity assignments suggested previously [11], were based on the possible proton-neutron SM configuration (see Sec. IV). A possible β decay of ^{137}Te to ^{137}I is expected to be primarily originated from the conversion of a neutron from the $f_{7/2}$ orbital into a proton in the $g_{7/2}$ (or $d_{5/2}$) orbital by a first-forbidden transition, thus in agreement with spin-parity of ^{137}Te g.s. of $7/2^-$. The feeding to the g.s. of the daughter ^{137}I with log $ft = 5.7(1)$ and maximal I_β value of 47(10) indicates that it proceeds by a first-forbidden non-unique transition with $\Delta J = 0$ and $\Delta\pi$ = -1 [29]. This suggests spin-parity of $7/2^+$ in agreement with the suggested from systematics spin/parity [12, 13]. Three more levels with suggested spin/parity of $(7/2^+)$ could be identified in the level scheme with log ft values between 6.0 and 6.6.

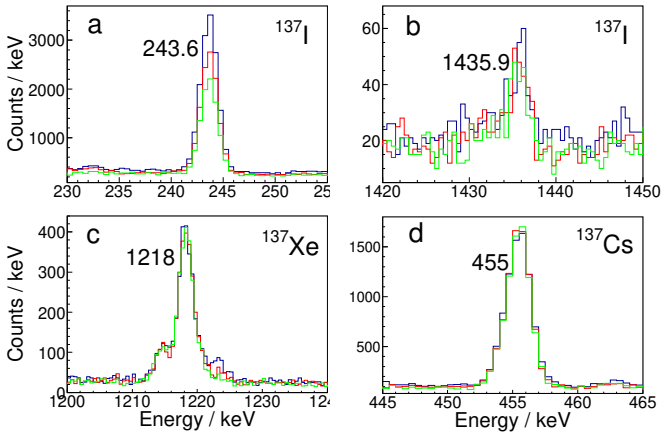

Figure 5. Energy spectrum corresponding to the decay of the nucleus chopped at each second. Blue, red and green (color online) are for the first 1^{st}, 2^{nd} and 3^{rd} second, respectively.

Other levels candidates e.g. with a log ft 6.9(1) and a smaller I_β of 2.4-2.8, possibly correspond to $\Delta J = 1, 2$ for these, spin/parity of $(3/2^+, 5/2^+)$ would be more appropriate. For about six levels with log ft ranging from 6.2 to 7.1, we propose the spin/parity of $(5/2^+)$ to be the most suitable candidate. In addition, based on the I_β branching, possible spins and multipolarities it may be assumed that some levels are candidates for $\Delta J = 2$ which suggests some uniqueness when appropriate as marked in Table II.

The proposed level scheme from this work is illustrated in Fig.7. Nine new levels (with one tentative among them) with 18 new transitions (with 2 tentative) are added to the revised previous knowledge. The tentative γ rays with 600 and 2047 keV energy which are hardly distinguishable in β-delayed γ-ray spectrum of ^{137}I are placed as they appear in gated spectrum and, moreover, fit the energy differences between already established levels.

E. P_n branch

Since the S_n of ^{137}Te is 2950(3) keV, within the $Q_\beta-$ window of Q_β =7053(9) keV [25, 30], β-delayed neutron emission is possible for the decay of the ^{137}Te nucleus. To obtain the β-delayed neutron emission probability, P_n, of ^{137}Te, we consider the known β decay of ^{136}Te [7]. The known γ-rays in ^{136}I are regarded with the same criteria as for transitions in

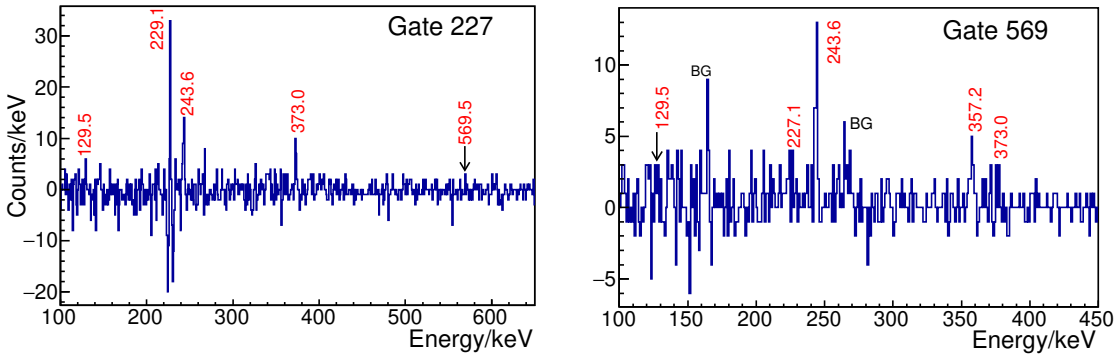

Figure 6. Coincidence γ-ray spectra gated on the 247 keV and 569 keV transitions. All marked peaks are in mutual coincidence.

^{137}I. Only one state at 87.3(7) keV with single transition to the g.s. is observed in this work. The resulting P_n amounts to 2.17(66)%, compared to the latest literature value of 2.6(3)% and the evaluated database value of 2.91(16)% in Ref. [31] may be regarded as lower limit for the knowledge of this quantity.

IV. SHELL-MODEL CALCULATIONS AND DISCUSSION

The experimental results are compared to theoretical calculations from large-scale shell-model calculations (SM) calculations. The $r4h - r5i$ model space with the ^{132}Sn nucleus as a core is used. The model-space, thus, consists of the entire major shell $1f_{7/2}$,$0h_{9/2}$,$1f_{5/2}$,$2p_{3/2}$, $2p_{1/2}$,$0i_{13/2}$ orbitals for neutrons and $0g_{7/2}$,$1d_{5/2}$,$1d_{3/2}$,$2s_{1/2}$, $0h_{11/2}$ orbitals for protons. Single-particle energies for neutrons and protons are taken from experimentally known data on ^{133}Sn and ^{133}Sb nuclei [32]. The $0i_{13/2}$ neutron and $2s_{1/2}$ proton orbital energies are inferred from Ref. [33] and Ref. [34], respectively. The N3LOP effective interaction [35] is used in this work. It was already demonstrated in several articles to successfully describe the spectroscopic properties and collectivity of nuclei in the region beyond ^{132}Sn, quoting as examples the Refs. [7, 8, 35–37]. The diagonalization of the considered system is achieved using the NATHAN shell-model code [38]. In this work, up to several excited states for the spin/parity/energy range of interest are calculated and compared to the proposed spin/parity assignments from the experiment in Fig. 8, the important main configurations for the positive (+) parity states are listed in Table III.

For the states of interest, illustrated in Fig. 8, also the main SM configurations are noted. The probable correspondence, whenever possible, may also be seen (with the color code).

It is interesting to remark immediately that for these states, the configuration is dominated by the proton configurations and, especially, the presence of the $d_{5/2}$ proton in the very close vicinity of the $g_{7/2}$ proton, inferred from the main occupation of these orbitals. Almost no neutron excitations are found to take place in the detailed analysis of the wave functions for the examined states, even for the highest in excitation energy. Note that reviewing higher-lying states would not be relevant to the observed experimental data. The details of the main configurations for ^{137}I may be traced for the computed states in Tab. III. This is certainly very different from the observed sequences in the ^{136}I neighbour, where various neutron excitations could be seen [7], including some moderate $\nu i_{13/2}$ occupation (see e.g. Fig. 13). Such behaviour may be attributed to the proximity of the $N = 82$ closed shell in the former case, to the fast step with the extra neutrons from an odd-odd to an odd-even system and finally to its structure.

As it can be seen from the current Table, the purity of the two main configurations in the low-energy states of ^{137}I is not small and, therefore, the other contributions appear with relatively minor weight in the wave functions. We present these results in accordance with the excited states that are candidates for the experimentally-populated spin/parity. In the Table, we give up to 10 excited states for the $3/2^+$ candidates for populated states at intermediate energy, and up to 6 excited states, as relevant for the spin/parities $5/2^+$, $7/2^+$, $9/2^+$, $11/2^+$ and $13/2^+$ (see Fig. 8). One may remark, that the neutron excitation to the $\nu p_{3/2}$ orbital is applicable only in a very few cases. The proton excitations containing the $\pi d_{5/2}$ orbital shows clearly a competition with the $\pi g_{7/2}$ orbital for excited states, and is also the second important contribution (with about 20%) in the $7/2^+$ g.s. of ^{137}I.

Another important point is the very small contribution of the $\nu h_{9/2}$ orbital in the wave function of the $7/2^-$ g.s. of the mother ^{137}Te nucleus. The presence of this $\nu h_{9/2}$ component and its decay to a state with $\pi h_{11/2}$ component in the daughter is the main responsible transition for a GT strength at the beginning of this major shell. In the neighbouring ^{136}I case, several 1^+ states originated from such main configuration are populated, with one very strong branch, as predicted by the SM at about 2 MeV excitation energy [7]. Similar range is recently suggested also for ^{138}I in Ref. [39]. Here, for $A = 137$, the $\nu h_{9/2}$ component is really minor with a theoretically calculated proportion of only 2.5%. Note, that while present in $A = 136$ with about 10%, it is completely blocked e.g. for ^{135}I. It is worth to highlight, that for $A = 140$ of the same isotopic chain (^{140}I), this probability is again enhanced with respect to $A = 137$, based on the more mixed g.s. configuration on one side and due to the lowered excitation energy of the GT states themselves, on the other, as it can be seen from the results in Ref. [40].

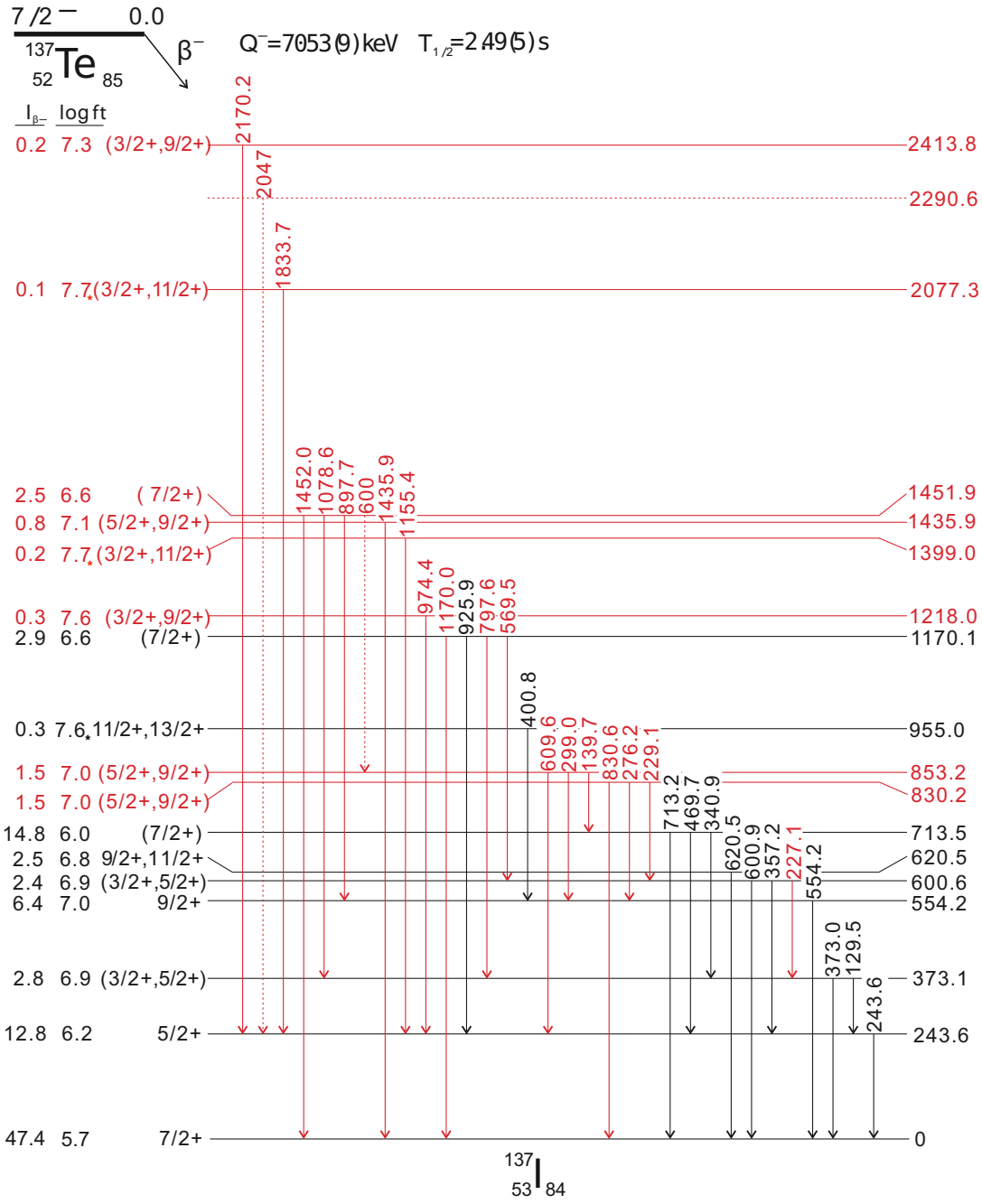

Figure 7. The proposed level scheme of ^{137}I obtained from β decay of ^{137}Te. The new levels and transitions are in red (color online), tentative transitions are with dotted line. The Q(β^-) of ^{137}Te is taken from Ref. [25]. For the levels marked with (*), some assumption for uniqueness may be possible (see text, Table II).

While reporting on the first excites states in the ^{137}Te mother nucleus, in Ref. [28], some $\nu h_{9/2}(f^2_{7/2})$ contributions are accounted e.g. for the yrast $9/2^-$ states, including the g.s. together with the three valence $\nu f^3_{7/2}$ configuration. These, as well as core vibrations coupled to them, were suggested to originate the $3/2^-$ and $5/2^-$ states, however they were not observed in the same study, while the position of these states is relevant in the situation of ^{137}Te nucleus. These states could be seen only in the more recent β-decay of ^{137}Sb $\rightarrow$^{137}Te [21], where the first negative parity states, expected with such configurations are found at relatively high in energy and thus not among those populated in the experimental β-decay results. It could, therefore, be concluded that at $A = 137$ no allowed branch $\nu h_{9/2} \rightarrow \pi h_{11/2}$ could be experimentally observed. As such contribution to the expected configurations is minor also in the examined ^{137}Te$\rightarrow$^{137}I study here, and none of the excited states seem to present such a strong transition branching, we

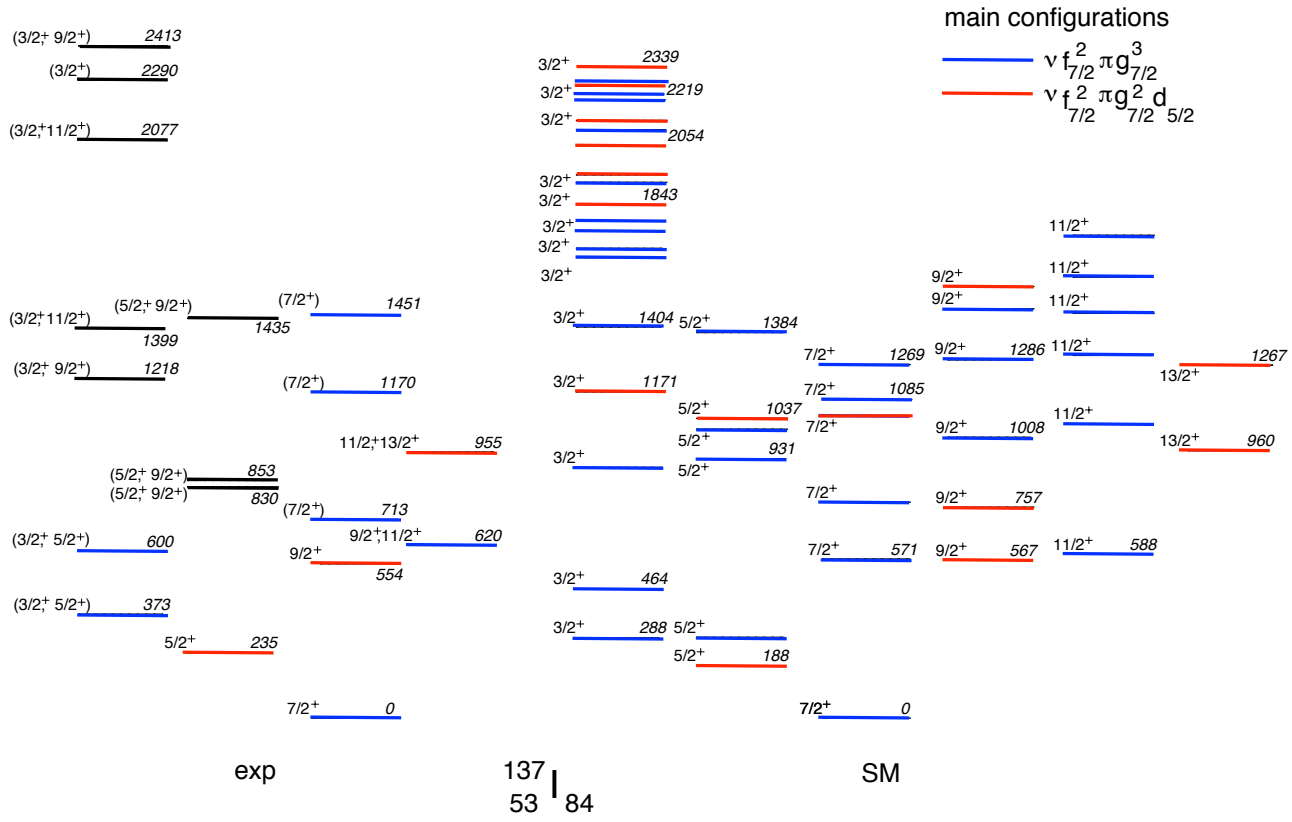

Figure 8. Experimental levels in ^{137}I compared to the theoretical shell-model (SM) calculations. The color code (online) indicates the main theoretical configurations and some of the possible experimental correspondences.

give similar conclusions for this odd$-A$ β decay.

A. The 7/2$^-$ g.s. of ^{137}Te

The g.s. spin/parity of the β-decaying ^{137}Te nucleus can rather firmly be set to 7/2$^-$ based on the experimental log ft values in the $A = 137$ I daughter and very strong branch to its 7/2$^+$ g.s. The direct g.s. to g.s. feeding is also relatively strong in this nucleus with about 47%. It behaves completely analogous to the $A = 135$ nucleus with similar experimental strength [12], from where similar spin/parities can be concluded.

The g.s. of ^{137}Te was suggested with quite some certitude in Ref. [11] based on the observation of a large part of its yrast scheme (up to spin/parity of (33/2$^+$)), multipolarity of several transitions connecting with the g.s. and SM calculations based on the Kuo-Herling (KH5082) [41] interaction, reasonably describing ^{137}I as the one proton coupling to the ^{136}Te nucleus. The perfect match of this assignment for the ^{137}I ($Z = 53, N = 84$) isotope to systematics of heavier-Z Cs, La isotone nuclei is found in a follow-up fission work [42], where the entire excitation scheme could be built in a complete analogy to the ^{139}Cs ($Z = 55, Z = 84$) isotone and in agreement with the data on other N=85 isotones [43]. These excitations are found also to be well described by the two-body CD-Bonn SM interaction using experimental single-particle energies from ^{133}Sb and ^{133}Sn nuclei [1].

Both mother and daughter $A = 137$ g.s. spin/parity assignments are in a good agreement also with our SM calculations using the N3LOP effective interaction. They predict the 7/2$^-$ state to be the ^{137}Te g.s.. It is already reported, that this prediction for lowest state with largest probability (>50%) as a single neutron state is in a full consistency with the Napoli SM interaction [21].

It is worth to note that similar predictions were given also in earlier works [28], where the 7/2$^-$ assignment is compared to systematics of the heavier isotones (up to $Z = 64$) and concluded that it is best choice for this $Z = 52$ nucleus. Also, it is quoted in Ref. [28] that this would suite the non-observation (in their data) of candidates for the 3/2$^-$ and 5/2$^-$ states for this nucleus. These candidates could only be tentatively suggested from β-decay to ^{137}Te to be at excitation energy of 61.8 keV for the (5/2$^-$) state and at least 1136.6 keV for some possible (3/2$^-$) state [21], despite the fact that this is somewhat in variance with the SM theory with both N3LOP and Napoli interactions, predicting the two states as first excited states at around the g.s. for N3LOP and around 200 keV for the Napoli SM interactions.

Table III. Main wave-function compositions for the positive (+) parity states of interest as predicted by the SM calculations for ^{137}I.

$\mathbf{J}_i^\pi$	Configuration-I	%	Configuration-II	%
$3/2^+_1$	$\pi(g^3_{7/2})\nu(f^2_{7/2})$	15	$\pi(g_{7/2}d^2_{5/2})\nu(f^2_{7/2})$	11
$3/2^+_2$	$\pi(g^3_{7/2})\nu(f^2_{7/2})$	13	$\pi(g^2_{7/2}d_{5/2})\nu(f^2_{7/2})$	11
$3/2^+_3$	$\pi(g^3_{7/2})\nu(f^2_{7/2})$	26	$\pi(g^2_{7/2}d_{3/2})\nu(f^2_{7/2})$	11
$3/2^+_4$	$\pi(g^2_{7/2}d_{5/2})\nu(f^2_{7/2})$	17	$\pi(d^3_{5/2})\nu(f^2_{7/2})$	12
$3/2^+_5$	$\pi(g^3_{7/2})\nu(f^2_{7/2})$	42	$\pi(g^2_{7/2}d_{5/2})\nu(f^2_{7/2})$	7
$3/2^+_6$	$\pi(g^3_{7/2})\nu(f^2_{7/2})$	34	$\pi(g^2_{7/2}d_{5/2})\nu(f^2_{7/2})$	12
$3/2^+_7$	$\pi(g^3_{7/2})\nu(f^2_{7/2})$	39	$\pi(g_{7/2}d^2_{5/2})\nu(f^2_{7/2})$	13
$3/2^+_8$	$\pi(g^3_{7/2})\nu(f^2_{7/2})$	17	$\pi(g^2_{7/2}d_{5/2})\nu(f^2_{7/2})$	17
$3/2^+_9$	$\pi(g^3_{7/2})\nu(f^2_{7/2})$	31	$\pi(g^2_{7/2}d_{5/2})\nu(f^2_{7/2})$	9
$3/2^+_{10}$	$\pi(g^2_{7/2}d_{5/2})\nu(f^2_{7/2})$	27	$\pi(g^3_{7/2})\nu(f^2_{7/2})$	12
$5/2^+_1$	$\pi(g^2_{7/2}d_{5/2})\nu(f^2_{7/2})$	41	$\pi(g^2_{7/2}d_{5/2})\nu(f_{7/2}p_{3/2})$	8
$5/2^+_2$	$\pi(g^3_{7/2})\nu(f^2_{7/2})$	33	$\pi(g^2_{7/2}d_{5/2})\nu(f^2_{7/2})$	9
$5/2^+_3$	$\pi(g^3_{7/2})\nu(f^2_{7/2})$	26	$\pi(g_{7/2}d^2_{5/2})\nu(f^2_{7/2})$	12
$5/2^+_4$	$\pi(g^3_{7/2})\nu(f^2_{7/2})$	32	$\pi(g_{7/2}d^2_{5/2})\nu(f^2_{7/2})$	17
$5/2^+_5$	$\pi(g^2_{7/2}d_{5/2})\nu(f^2_{7/2})$	23	$\pi(g^3_{7/2})\nu(f^2_{7/2})$	16
$5/2^+_6$	$\pi(g^3_{7/2})\nu(f^2_{7/2})$	30	$\pi(g^2_{7/2}d_{5/2})\nu(f^2_{7/2})$	22
$7/2^+_1$	$\pi(g^3_{7/2})\nu(f^2_{7/2})$	31	$\pi(g_{7/2}d^2_{5/2})\nu(f^2_{7/2})$	19
$7/2^+_2$	$\pi(g^3_{7/2})\nu(f^2_{7/2})$	18	$\pi(g_{7/2}d^2_{5/2})\nu(f^2_{7/2})$	17
$7/2^+_3$	$\pi(g^3_{7/2})\nu(f^2_{7/2})$	23	$\pi(g^2_{7/2}d_{5/2})\nu(f^2_{7/2})$	22
$7/2^+_4$	$\pi(g^2_{7/2}d_{5/2})\nu(f^2_{7/2})$	29	$\pi(g^3_{7/2})\nu(f^2_{7/2})$	22
$7/2^+_5$	$\pi(g^3_{7/2})\nu(f^2_{7/2})$	40	$\pi(g^2_{7/2}d_{5/2})\nu(f^2_{7/2})$	11
$7/2^+_6$	$\pi(g^3_{7/2})\nu(f^2_{7/2})$	35	$\pi(g^2_{7/2}d_{5/2})\nu(f^2_{7/2})$	16
$9/2^+_1$	$\pi(g^2_{7/2}d_{5/2})\nu(f^2_{7/2})$	17	$\pi(g^3_{7/2})\nu(f^2_{7/2})$	12
$9/2^+_2$	$\pi(g^2_{7/2}d_{5/2})\nu(f^2_{7/2})$	26	$\pi(g^2_{7/2}d_{5/2})\nu(f_{7/2}p_{3/2})$	13
$9/2^+_3$	$\pi(g^3_{7/2})\nu(f^2_{7/2})$	44	$\pi(g_{7/2}d^2_{5/2})\nu(f^2_{7/2})$	10
$9/2^+_4$	$\pi(g^3_{7/2})\nu(f^2_{7/2})$	46	$\pi(g_{7/2}d^2_{5/2})\nu(f^2_{7/2})$	10
$9/2^+_5$	$\pi(g^3_{7/2})\nu(f^2_{7/2})$	33	$\pi(g_{7/2}d^2_{5/2})\nu(f^2_{7/2})$	11
$9/2^+_6$	$\pi(g^2_{7/2}d_{5/2})\nu(f^2_{7/2})$	28	$\pi(g_{7/2}d^2_{5/2})\nu(f^2_{7/2})$	12
$11/2^+_1$	$\pi(g^3_{7/2})\nu(f^2_{7/2})$	23	$\pi(g_{7/2}d^2_{5/2})\nu(f^2_{7/2})$	15
$11/2^+_2$	$\pi(g^3_{7/2})\nu(f^2_{7/2})$	20	$\pi(g_{7/2}d^2_{5/2})\nu(f^2_{7/2})$	15
$11/2^+_3$	$\pi(g^3_{7/2})\nu(f^2_{7/2})$	31	$\pi(g^2_{7/2}d_{5/2})\nu(f^2_{7/2})$	16
$11/2^+_4$	$\pi(g^3_{7/2})\nu(f^2_{7/2})$	51	$\pi(g_{7/2}d^2_{5/2})\nu(f^2_{7/2})$	10
$11/2^+_5$	$\pi(g^3_{7/2})\nu(f^2_{7/2})$	30	$\pi(g^2_{7/2}d_{5/2})\nu(f^2_{7/2})$	22
$11/2^+_6$	$\pi(g^3_{7/2})\nu(f^2_{7/2})$	24	$\pi(g^2_{7/2}d_{5/2})\nu(f^2_{7/2})$	23
$13/2^+_1$	$\pi(g^2_{7/2}d_{5/2})\nu(f^2_{7/2})$	20	$\pi(g^3_{7/2})\nu(f^2_{7/2})$	13
$13/2^+_2$	$\pi(g^2_{7/2}d_{5/2})\nu(f^2_{7/2})$	31	$\pi(g^3_{7/2})\nu(f^2_{7/2})$	14

B. Origin of new new positive-parity states in ^{137}I

The appearance of the possible ($3/2^+$) states is uniquely identified in this work (see Fig.7). These states appear in the neighbouring ^{135}I where the g.s. spin/parity is the same as in the other odd$-A$ I isotopes, including $A = 137$. These states cover several possibilities in $A = 135$ with log ft around 7.4-7.5 and together with the $11/2^+$ possibilities up to 8.1 [12]. The candidates in $A = 137$, again similarly probable, cover except possible $\Delta J = 2$ (of the g.s.) also $\Delta J = 1$ and together with the spin/parity of $11/2^+$, cover log ft values from 6.8 to 7.7. For three of the observed states with $\Delta J = 2$ as most probable scenario, also uniqueness of the first-forbidden transitions may be assumed, reflecting the upper log ft value as given in Table II.

It is the position of the $3/2^+$ states that is well matching the predicted excitation energy by the SM calculations. It can be seen in Fig. 8, where the direct correspondence and the predicted configuration as part of the $\nu f^2_{7/2}\pi g^3_{7/2}$ multiplet may be traced. The competing $\pi d_{5/2}$ configuration is relevant only for states above 1.1 MeV and some of the higher-lying in energy experimental candidates that, nevertheless, may correspond to a theoretical state with such origin (see color code, online). However, some of the other propositions for these states as $5/2^+$, $9/2^+$ (or $11/2^+$) also predicted nearby would finally not be excluded.

Of the $11/2^+$ states, only those with the lowest $\nu f^2_{7/2}\pi g^3_{7/2}$ configuration (see Table III) may be seen. Indeed, the lowest of these states being among the experimental possibilities (E_x = 620 keV) has a remarkable theoretical (E_x = 588 keV) correspondence. The experimental possibilities for the second and third $11/2^+$ states listed together with the first $13/2^+$ or fifth $3/2^+$ possibilities, respectively, have also perfect SM counterparts.

Concerning the $5/2^+$ states, we could classify with certitude the first excited states of them, which is based as expected, on the predominant $\pi d_{5/2}$ configuration (see Table III with more than 40% probability). As it stays only at E_x = 235 keV, the orbital positioning may be inferred, and compared with other recent data with similar conclusions [4, 7, 21]. Moreover, this state is reported also in the heavier ^{139}I at E_x = 208 keV and compared to the same SM prediction (E_x = 175 keV) with rather good agreement [5, 8]. It can be, therefore, concluded that no drastic change it the $\pi d_{5/2}$ orbital is present in these I isotopes, which is different than its behaviour of the Sb isotopes [4, 21]. Interestingly, in the $A = 135$ Iodine neighbour, the second $5/2^+$ state is also observed in the vicinity of the first (e.g. at about 270 keV excitation energy difference) [12]. This is the predicted by the SM appearance in ^{137}I (see Fig. 8). We have observed another candidate within the excitation energy, e.g. the 373.1 keV state, however it may also be assigned differently. The clear difference is based on the experimentally observed I_β and respective log ft values that for the $5/2^+$ state in our work amount to 12.8 and 6.2, respectively. It is in a very good agreement with the data on both $5/2^+$ states in ^{135}I, with respective values of 24.2/16.4 and 6.3/6.4. In ^{137}I, two $5/2^+$ states with $d_{5/2}$ proton are predicted among the first six in about 1 MeV energy spacing, thus larger than in the lighter neighbour. Indeed, two candidates can be traced among the excited states around 850 keV and 1.4 MeV (see Fig. 7).

Similar is the situation with the $9/2^+$ states, two of which are based on the same proton excitation as the $5/2^+$ states, while the rest belong to the $\nu f^2_{7/2}\pi g^3_{7/2}$ multiplet. It has to be underlined, however, that their wave-functions are much more mixed than those of the $5/2^+$ states with relative contributions of the order of 17%. Experimentally, only the first $9/2^+$ is firmly assigned, while the other six candidates ($\Delta J = 1$ of the

g.s.) are in competition (with the possible $5/2^+$ assignment for three of the states, or due to β branching also to pairs of states with other possible ($3/2^+$ and $11/2^+$) assignment, even if the most probable transition multipolarities are considered. Based on the enhanced branch to the first $7/2^+$ state and the predicted second SM state e.g. one may suggest for the 830-keV state more a probable $9/2^+$ than $5/2^+$ attribution, while for the higher lying ones such scenario may be relatively uncertain.

The most strongly fed $7/2^+$ states from the direct feeding of the $7/2^-$ g.s. state are naturally in a good agreement with the $J = 7/2$ assignments. Any other different spin/parity would not present these strong branches well visible in the level scheme (Fig. 7) and this certainly excludes the $J = 5/2$ for the g.s. as e.g. the feeding to the 243.6 keV and 713.5 keV states is clearly different. The log ft values of the newly identified ($7/2^+$) states are also of the order of 6 and the first excited after the g.s. seems very likely at 713.5 keV excitation energy, based on these experimentally established I_β feeding, although slightly underestimated in energy by the theory (Fig. 8). Interestingly, in the earlier β decay work, mostly the assigned as $7/2^+$ states are observed and where the next such candidate, previously set but unassigned at 1169.0 keV [12], is confirmed here at 1170.0 keV. In this work, we propose one more candidate for $7/2^+$ at 1.4 MeV excitation energy (Fig. 8). These states are purely based on the proton $g^3_{7/2}$ configuration with the exception of the slightly competing $\pi g^2_{7/2} d_{5/2}$ contribution for the $7/2^+_2$ state and their theoretical correspondence is relatively good as it can be seen in the Figure.

As stated earlier, the non-observation of states containing GT strength, confirms that this channel is still blocked for ^{137}I nucleus and that the decay of the ^{137}Te is completely dominated by the first-forbidden transitions from the dominating $\nu f^3_{7/2} \pi g^2_{7/2}$ g.s. This is in full agreement with the SM calculations that also do not expect such branching at low energy and the first possible transition between the $7/2^-$ (^{137}Te) $\rightarrow$ $5/2^-$ (^{137}I) is expected at $E_x(5/2^-)$=3.8 MeV with $B(GT)$ of about 0.007, which is not found experimentally. It would be further interesting to investigate whether this strength can again be unblocked e.g. due the expectations of more mixing and an evolving collectivity also in the heavier neighbours.

V. SUMMARY

In this work, we performed new β-decay spectroscopy of the ^{137}Te nucleus to the daughter ^{137}I. We observed several new transitions corresponding to first-forbidden branches to excited states in ^{137}I. Due to the relatively weak P_n ratio and insufficient statistics, the transitions after β-delayed neutron emission were strongly hindered and only few indications of states in ^{137}I could be seen. Therefore, such investigation would require more experimental data.

From the investigations performed in this work, it is interesting to highlight the non-observation of GT strength for this $A = 137$ isotope, while a possible even-odd effect with decrease of the GT strength at the expense of favoured first-forbidden decay seems to be present. Furthermore, the strong effect of both $\pi g_{7/2}$ and $\pi d_{5/2}$ proton orbitals seems to completely dominate the structure of the ^{137}I isotope observed in our data up to 2.4 MeV excitation energy.

The nucleus has an interesting relation to studies of electron and anti-neutrino reactor spectral behaviour in connection to the role of the first-forbidden transitions, especially as forbidden decays cannot be neglected and need to be accounted properly. Being an essential ingredient in the understanding not only for nuclear astrophysics but also reactor anti-neutrino spectra, these type of studies certainly merit deeper investigation.

ACKNOWLEDGMENTS

The authors would like to thank the ILL staff for providing good quality neutron beam, the support of N. Laurens and the engineering team of Lohengrin for their help in mounting the experimental setup and handle during the long experiment. The usage of EXOGAM Clovers together with their respective Anti-Compton shields from GANIL is also acknowledged. The fund support No.201804910510 provided by China Scholarship Council (CSC) is acknowledged.

[1] L. Coraggio, A. Covello, A. Gargano, N. Itaco, and T. Kuo, Prog. Part. Nucl. Phys. **62**, 135 (2009).
[2] A.B. Brown, Phys. Rev. Lett. **85**, 5296 (2000).
[3] J. Shergur, B. A. Brown, V. Fedoseyev, U. Köster, K.-L. Kratz, D. Seweryniak, W. B. Walters, A. Wöhr, D. Fedorov, M. Hannawald, M. Hjorth-Jensen, V. Mishin, B. Pfeiffer, J. J. Ressler, H. O. U. Fynbo, P. Hoff, H. Mach, T. Nilsson, K. Wilhelmsen-Rolander, H. Simon, A. Bickley, and the ISOLDE Collaboration, Phys. Rev. C **65**, 034313 (2002).
[4] R. Lozeva, H. Naïdja, F. Nowacki, J. Dudek, A. Odahara, C.-B. Moon, S. Nishimura, P. Doornenbal, J.-M. Daugas, P.-A. Söderström, T. Sumikama, G. Lorusso, J. Wu, Z. Y. Xu, H. Baba, F. Browne, R. Daido, Y. Fang, T. Isobe, I. Kojouharov, N. Kurz, Z. Patel, S. Rice, H. Sakurai, H. Schaffner, L. Sinclair, H. Watanabe, A. Yagi, R. Yokoyama, T. Kubo, N. Inabe, H. Suzuki, N. Fukuda, D. Kameda, H. Takeda, D. S. Ahn, D. Murai, F. L. Bello Garrote, F. Didierjean, E. Ideguchi, T. Ishigaki, H. S. Jung, T. Komatsubara, Y. K. Kwon, P. Lee, C. S. Lee, S. Morimoto, M. Niikura, H. Nishibata, and I. Nishizuka, Phys. Rev. C **93**, 014316 (2016).
[5] W. Urban, T. Rzaca-Urban, A. Korgul, J. L. Durell, M. J. Leddy, M. A. Jones, W. R. Phillips, A. G. Smith, B. J. Varley, I. Ahmad, L. R. Morss, and N. Schulz, Pays. Rev. C **65**, 024307 (2002).
[6] G. Häfner, R. Lozeva, H. Naďja, M. Lebois, N. Jovancevic, D. Thisse, D. Etasse, R. L. Canavan, M. Rudigier, J. N. Wilson, E. Adamska, P. Adsley, M. Babo, K. Belvedere, J. Benito, G. Benzoni, A. Blazhev, A. Boso, S. Bottoni, M. Bunce, R. Chakma, N. Cieplicka-Orynczak, S. M. Collins, M. L. Cortés, P. J. Davies, C. Delafosse, M. Fallot, B. Fornal, L. M. Fraile, R.-B. Gerst, D. Gjestvang, V. Guadilla, K. Hauschild, C. Hen-

rich, I. Homm, F. Ibrahim, L. W. Iskra, S. Jazwari, J. Jolie, A. Korgul, P. Koseoglou, Th. Kröll, T. Kurtukian-Nieto, L. Lemeur, J. Ljungvall, A. Lopez-Martens, I. Matea, L. Matthieu, K. Miernik, J. Nemer, S. Oberstedt, W. Paulsen, M. Piersa, Y. Popovitch, C. Porzio, L. Qi, D. Ralet, P. H. Regan, D. Reygadas Tello, K. Rezynkina, V. Sanchez, C. Schmitt, P.-A. Söderström, C. Sürder, G. Tocabens, V. Vedia, D. Verney, N. Warr, B. Wasilewska, J. Wiederhold, M. S. Yavahchova, F. Zeiser, and S. Ziliani, Phys. Rev. C **103**, 034317 (2021).

[7] R. Lozeva, E. A. Stefanova, H. Naïdja, F. Nowacki, T. Rzaca-Urban, J. Wisniewski, W. Urban, I. Ahmad, A. Blanc, G. De France, F. Didierjean, G. Duchêne, H. Faust, J. P. Greene, U. Köster, P. Mutti, G. Simpson, A. G. Smith, T. Soldner, and C. A. Ur, Phys. Rev. C **98**, 024323 (2018).

[8] G. Häfner, R. Lozeva, H. Naïdja, M. Lebois, N. Jovancevic, D. Thisse, D. Etasse, R. L. Canavan, M. Rudigier, J. N. Wilson, E. Adamska, P. Adsley, A. Algora, M. Babo, K. Belvedere, J. Benito, G. Benzoni, A. Blazhev, A. Boso, S. Bottoni, M. Bunce, R. Chakma, N. Cieplicka-Orynczak, S. M. Collins, M. L. Cortés, P. J. Davies, C. Delafosse, M. Fallot, L. M. Fraile, R.-B. Gerst, D. Gjestvang, V. Guadilla, K. Hauschild, C. Henrich, I. Homm, F. Ibrahim, L. W. Iskra, S. Jazwari, A. Korgul, P. Koseoglou, Th. Kröll, T. Kurtukian-Nieto, L. Lemeur, S. Leoni, J. Ljungvall, A. Lopez-Martens, L. Matthieu, K. Miernik, J. Nemer, S. Oberstedt, W. Paulsen, M. Piersa-Silkowska, Y. Popovitch, C. Porzio, L. Qi, D. Ralet, P. H. Regan, D. Reygadas Tello, K. Rezynkina, V. Sanchez-Tembleque, C. Schmitt, P.-A. Söderström, C. Sürder, G. Tocabens, V. Vedia, D. Verney, N. Warr, B. Wasilewska, J. Wiederhold, M. S. Yavahchova, F. Zeiser, and S. Ziliani, Phys. Rev. C **104**, 014316 (2021).

[9] V. Paar, Phys. Lett. B **39**, 466 (1972).

[10] G.V. Berghe, Z. Phys. **266**, 139 (1974).

[11] A. Korgul, W. Urban, T. Rzaca-Urban, M. Górska, JL. Durell, M.J. Leddy, M.A. Jones, WR. Phillips, A.G. Smith, BJ. Varley, M. Bentaleb, E. Lubkiewicz, N. Schulz, I. Ahmad, and L.R. Morss, Eur.Phys. Journ. A **12**, 129 (2001).

[12] M. Samri, G.J. Costa, G. Klotz, D. Magnac, R. Seltz, and J.P. Zirnheld, Z. Phys. A **321**, 255 (1985).

[13] E. Browne and J.K. Tuli, Nucl. Dat. Sh. **108**, 2173 (2007).

[14] J. Vervier, J. Aysto, H. Doubre, S. Gales, G. Morrison, G. Ricco, D. Schwalm, and G.E. Korner, NuPECC report-December 1997 (1997).

[15] J. Vervier, Nucl. Phys. N. **10**, 27 (2000).

[16] R. Bennett, P. van Duppen, H. Geissel, K. Heyde, B. Jonson, O. Kester, G.E. Koerner, W. Mittig, A.C. Mueller, G. Muenzenberg, *et al.*, (2000).

[17] P. Armbruster, M. Asghar, J.P. Bocquet, R. Decker, H. Ewald, J. Greif, E. Moll, B. Pfeiffer, H. Schrader, F. Schussler, G. Siegert, and H. Wollnik, J. Phys. **139**, 213 (1976).

[18] L. Mathieu, O. Serot, T. Materna, A. Bail, U. Köster, H. Faust, O. Litaize, E. Dupont, C. Jouanne, A. Letourneau, *et al.*, J. Instrum. **7**, P08029 (2012).

[19] M. Si, R. Lozeva, H. Naïdja, A. Blanc, J.-M. Daugas, F. Didierjean, G. Duchêne, U. Köster, T. Kurtukian-Nieto, F. Le Blanc, P. Mutti, M. Ramdhane, and W. Urban, Phys. Rev. C (2022).

[20] R. Thibes and S. L. de Oliveira, Int. J. P. Appl. Math. **93**, 879 (2014).

[21] B. Moon, A. Jungclaus, H. Naïdja, A. Gargano, R. Lozeva, C.-B. Moon, A. Odahara, G. S. Simpson, S. Nishimura, F. Browne, P. Doornenbal, G. Gey, J. Keatings, G. Lorusso, Z. Patel, S. Rice, M. Si, L. Sinclair, P.-A. Söderström, T. Sumikama, J. Taprogge, H. Watanabe, J. Wu, Z. Y. Xu, A. Yagi, D. S. Ahn, H. Baba, F. L. Bello Garrote, S. Bönig, R. Daido, J. M. Daugas, F. Didierjean, F. Drouet, Y. Fang, N. Fukuda, R. Gernhäuser, B. Hong, E. Ideguchi, S. Ilieva, N. Inabe, T. Ishigaki, T. Isobe, H. S. Jung, D. Kameda, I. Kojouharov, T. Komatsubara, T. Kröll, T. Kubo, N. Kurz, Y. K. Kwon, C. S. Lee, P. Lee, Z. Li, A. Montaner-Pizá, S. Morimoto, K. Moschner, D. Mücher, D. Murai, M. Niikura, H. Nishibata, I. Nishizuka, R. Orlandi, H. Sakurai, H. Schaffner, Y. Shimizu, K. Steiger, H. Suzuki, H. Takeda, K. Tshoo, Zs. Vajta, A. Wendt, R. Yokoyama, and K. Yoshinaga, Phys. Rev. C **103**, 034320 (2021).

[22] O. Arndt, K.-L. Kratz, W. B. Walters, K. Farouqi, U. Köster, V. Fedosseev, S. Hennrich, C. J. Jost, A. Wöhr, A. A. Hecht, B. Pfeiffer, J. Shergur, and N. Hoteling, Phys. Rev. C **84**, 061307 (2011).

[23] M. Asghar, J.P. Gautheron, G. Bailleul, J.P. Bocquet, J. Greif, H. Schrader, G. Siegert, C. Ristori, J. Crancon, and G.I. Crawford, Nucl. Phys. A **247**, 359 (1975).

[24] J. Wu, S. Nishimura, P. Möller, M. R. Mumpower, R. Lozeva, C. B. Moon, A. Odahara, H. Baba, F. Browne, R. Daido, P. Doornenbal, Y. F. Fang, M. Haroon, T. Isobe, H. S. Jung, G. Lorusso, B. Moon, Z. Patel, S. Rice, H. Sakurai, Y. Shimizu, L. Sinclair, P.-A. Söderström, T. Sumikama, H. Watanabe, Z. Y. Xu, A. Yagi, R. Yokoyama, D. S. Ahn, F. L. Bello Garrote, J. M. Daugas, F. Didierjean, N. Fukuda, N. Inabe, T. Ishigaki, D. Kameda, I. Kojouharov, T. Komatsubara, T. Kubo, N. Kurz, K. Y. Kwon, S. Morimoto, D. Murai, H. Nishibata, H. Schaffner, T. M. Sprouse, H. Suzuki, H. Takeda, M. Tanaka, K. Tshoo, and Y. Wakabayashi, Phys. Rev. C **101**, 042801 (2020).

[25] M. Wang, W.J. Huang, F.G. Kondev, G. Audi, and S. Naimi, Chin. Phys. C **45**, 030003 (2021).

[26] M. Emeric and A. Sonzogni, "Calculation program of log ft," web (accessed 2021), `https://www.nndc.bnl.gov/logft/`.

[27] J. Agramunt, J.L. Tain, M.B. Gómez-Hornillos, A.R. Garcia, F. Albiol, A. Algora, R‘Ă‘Ć Caballero-Folch, F. Calviño, D. Cano-Ott, G. Cortés, *et al.*, Nucl. Instr. and Meth. A **807**, 69–78 (2016).

[28] W. Urban, A. Korgul, T. Rzaca-Urban, N. Schulz, M. Bentaleb, E. Lubkiewicz, J. L. Durell, M. J. Leddy, M. A. Jones, W. R. Phillips, A. G. Smith, B. J. Varley, I. Ahmad, and L. R. Morss, Phys. Rev. C **61**, 041301 (2000).

[29] S. Raman and N.B. Gove, Phys. Rev. C **7**, 1995 (1973).

[30] NNDC database, (accessed 2021), `https://www.nndc.bnl.gov`.

[31] J. Liang, B. Singh, E.A. McCutchan, I. Dillmann, M. Birch, A.A. Sonzogni, X. Huang, M. Kang, J. Wang, G. Mukherjee, *et al.*, Nucl. Dat. Sh. **168**, 1–116 (2020).

[32] Yu. Khazov, A. Rodionov, and F.G. Kondev, Nucl. Dat. Sh. **112**, 855 (2011).

[33] W. Urban, W. Kurcewicz, A. Nowak, T. Razca-Urban, J.L. Durell, M.J. Leddy, M.A. Jones, W.R. Phillips, A.G. Smith, B.J. Varley, M. Bentaleb, E. Lubkiewciz, N. Schulz, J. Blomqvist, P. J. Daly, P. Bhattacharyya, C.T. Zhang, I. Ahmad, and L.R. Morss, EPJ A **5**, 239 (1999).

[34] F. Andreozzi, L. Coraggio, A. Covello, A. Gargano, T.T.S. Kuo, and A. Porrino, Phys. Rev. C **56**, R16 (1997).

[35] H. Naïdja, F. Nowacki, and B. Bounthong, Phys. Rev. C **96**, 034312 (2017).

[36] H. Naïdja and F. Nowacki, EPJ Web Conf. **193**, 01005 (2018).

[37] H. Naïdja, F. Nowacki, B. Bounthong, M. Czerwinski, T. Rzaca-Urban, T. Roginski, W. Urban, J. Wisniewski, K. Sieja, A.G. Smith, J.F. Smith, G.S. Simpson, I. Ahmad, and J.P. Greene, Phys. Rev. C **95**, 064303 (2017).

[38] E. Caurier, G. Martínez-Pinedo, F. Nowack, A. Poves, and A. P. Zuker, Rev. Mod. Phys. **77**, 427 (2005).

[39] B. Moon, A. Gargano, H. Naïdja, C.-B. Moon, A. Odahara,

R. Lozeva, S. Nishimura, C. Yuan, F. Browne, P. Doornenbal, G. Lorusso, Z. Patel, S. Rice, M. Si, L. Sinclair, P.-A. Söderström, T. Sumikama, H. Watanabe, J. Wu, Z. Y. Xu, A. Yagi, *et al.*, Phys. Rev. C (2022).

[40] B. Moon, C.-B. Moon, A. Odahara, R. Lozeva, P.-A. Söderström, F. Browne, C. Yuan, A. Yagi, B. Hong, H. S. Jung, P. Lee, C. S. Lee, S. Nishimura, P. Doornenbal, G. Lorusso, T. Sumikama, H. Watanabe, I. Kojouharov, T. Isobe, H. Baba, H. Sakurai, R. Daido, Y. Fang, H. Nishibata, Z. Patel, S. Rice, L. Sinclair, J. Wu, Z. Y. Xu, R. Yokoyama, T. Kubo, N. Inabe, H. Suzuki, N. Fukuda, D. Kameda, H. Takeda, D. S. Ahn, Y. Shimizu, D. Murai, F. L. Bello Garrote, J. M. Daugas, F. Didierjean, E. Ideguchi, T. Ishigaki, S. Morimoto, M. Niikura, I. Nishizuka, T. Komatsubara, Y. K. Kwon, and K. Tshoo, Phys. Rev. C **96**, 014325 (2017).

[41] W.-T. Chou and E. K. Warburton, Phys. Rev. C **45**, 1720 (1992).

[42] S. H. Liu, J. H. Hamilton, A. V. Ramayya, A. Covello, A. Gargano, N. Itaco, Y. X. Luo, J. O. Rasmussen, J. K. Hwang, A. V. Daniel, G. M. Ter-Akopian, S. J. Zhu, and W. C. Ma, Phys. Rev. C **80**, 044314 (2009).

[43] W. Urban, W. R. Phillips, I. Ahmad, J. Rekawek, A. Korgul, T. Rzaca-Urban, J. L. Durell, M. J. Leddy, A. G. Smith, B. J. Varley, N. Schulz, and L. R. Morss, Pays. Rev. C **66**, 044302 (2002).